Dynamics of Carbonyl-Modified-Epoxy/Amine Networks by FTIR and Dielectric Relaxation Spectroscopy

Saša Andjelić and Jovan Mijović*

Department of Chemical Engineering, Chemistry and Materials Science, Polytechnic University, Six Metrotech Center, Brooklyn, New York 11201

Received June 5, 1998; Revised Manuscript Received October 1, 1998

ABSTRACT: An investigation was conducted to determine how the molecular architecture of prepolymers affects the dynamics of epoxy/amine networks at various stages of cross-linking. An epoxy prepolymer with a carbonyl group attached to the glycidyl ether moiety was utilized, in anticipation that the presence of the carbonyl group would have a specific affect on the interactions and dynamics in these networks. Experimental results were obtained in real time by simultaneous broad-band dielectric relaxation spectroscopy and near-infrared Fourier transform spectroscopy. An unusual increase in the relaxed (limiting low-frequency) dielectric constant was observed, and an explanation was offered in terms of an intramolecular hydrogen-bonded complex that co-involves carbonyl and hydroxyl groups. A pronounced change was also noted in the IR absorption of epoxy and carbonyl groups near the gel point and was assigned to specific dipolar interactions in the growing network. Frequency sweeps of reactive networks reveal initially the $\alpha\beta$ process at high frequency (peak at ca. 2 GHz). With the advancement of reactions, however, α and β relaxations begin to separate out; α relaxation shifts gradually to lower frequency as the glass transition of the growing network increases, while β relaxation, because of its localized origin, is little affected by the network growth. An unusual form of thermodielectric complexity is observed in the relaxation spectrum for the α process. Finally, building upon an earlier study by Fournier et al. (*Macromolecules* **1996**, *29*, 7097), a correlation between molecular dynamics and chemical kinetics during network formation is reported.

Introduction

Dynamics of glass formers are currently the subject of extensive experimental and theoretical research worldwide,[1] but only a small number of those studies have been performed on polymers that undergo a temporal evolution of structure as a result of chemical reaction, crystallization, or liquid crystallinity (e.g., refs 2−9). As a part of the comprehensive research program on reactive polymer networks, which is currently underway at Polytechnic University, we have recently reported the results of an investigation of the reorientational dynamics of epoxy/amine networks at various stages of cross-linking by simultaneous broad-band dielectric relaxation spectroscopy (DRS) and near-infrared spectroscopy (NIR).[10] We studied multifunctional epoxy/amine formulations based on diglycidyl ether of Bisphenol A, or DGEBA, and found that the variation in apparent activation energy (determined from the temperature dependence of the dielectric loss peak) as a function of the degree of cure was most informative. Three zones of dipole dynamics were identified: an initial zone where the activation energy increases with the degree of cure; an intermediate zone, between about 55 and 65% conversion, where the activation energy displays a peculiar trend; and a third zone where the activation energy decreases as cure approaches completion. We established that the unusual behavior in the intermediate zone was caused by chemical and physical changes in the growing network in the vicinity of gel point. More specifically, dipole dynamics were strongly affected by the formation and the subsequent breakup of three-dimensional hydrogen-bonded complexes that co-involve hydroxyl, epoxy, and amine groups.

In all epoxy prepolymers used in that study, the epoxy group that is at the origin of the dielectric α process was a part of the glycidyl ether moiety attached to a benzene ring, as illustrated in Figure 1A. Of interest in the present work was modification of the molecular structure of the epoxy prepolymer by (1) inserting a carbonyl group between the ether oxygen and the cyclohexyl ring and (2) replacing the benzene ring in DGEBA with a cyclohexyl ring. The resulting epoxy molecule, shown in Figure 1B, is known as diglycidyl 1,2-cyclohexanedicarboxylate, or DGCDC, and will be referred to throughout the text by this acronym. The next step was to study the effect of this new molecular architecture on (1) specific interactions and dipole dynamics during the network formation and (2) correlations between molecular dynamics and chemical kinetics during network formation. It was anticipated that the presence of a *carbonyl group* in the epoxy prepolymer would have a direct effect on the network dynamics for several reasons: (1) it should affect specific interactions in the reactive mixture and particularly the makeup of hydrogen-bonded complexes which form in the course of epoxy/amine cure; (2) it should affect the mean-square dipole moment because the dipole moment of an isolated ester group (1.89 D) is higher than that of the corresponding ether moiety (1.09 D);[11] (3) the polarity of the carbonyl group depends on the conformation energy about the cyclohexyl/carbonyl bond,[11] which should vary during cure and thus affect the mean-square dipole moment.

The principal objective of this study was to elucidate how a change in the molecular architecture of epoxy prepolymer affects the reorientational dynamics of epoxy/amine networks during cure. This was accomplished by using DRS and NIR to compare the dynamics

10.1021/ma980894w CCC: $15.00
Published on Web 11/11/1998

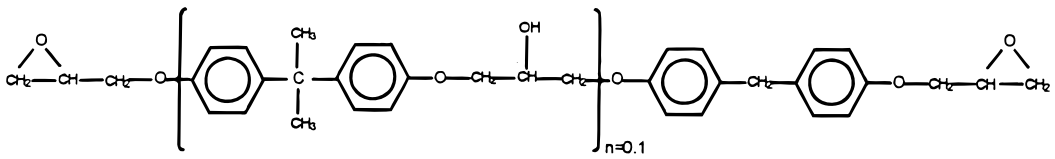

A

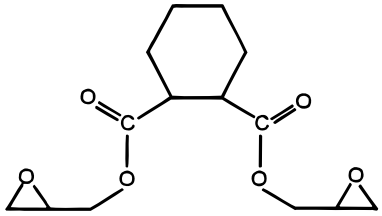

B

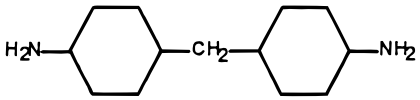

C

Figure 1. Chemical structures of (A) diglycidyl ether of Bisphenol A or DGEBA; (B) diglycidyl 1,2-cyclohexanedicarboxylate or DGCDC; and (C) 4,4′-methylenebis(cyclohexylamine) or PACM.

of networks based on DGEBA and DGCDC epoxy prepolymers during cure.

Experimental Section

Materials. The formulation studied was composed of DGCDC and 4,4′-methylenebis(cyclohexylamine) (PACM). Chemical structures of DGCDC and PACM are shown in parts B and C of Figure 1, respectively. Both chemicals were supplied by Aldrich and were used without further purification. The stoichiometric ratio of epoxy group and amine hydrogen was used, and tests were performed at different conditions of frequency, time, and temperature.

Techniques. a. Dielectric Relaxation Spectroscopy. Our experimental facility for dielectric measurements consists of commercial and custom-made (in-house) instruments that include a Solartron 1260 impedance/gain phase analyzer (10 μHz to 32 MHz), a Hewlett-Packard 4284A precision LCR meter (20 Hz to 1 MHz), a Hewlett-Packard 8752C network analyzer (300 kHz to 1.3 GHz), and a Hewlett-Packard 4291A RF impedance analyzer (1 MHz to 1.8 GHz). Each instrument is modified by the addition of a temperature-controlled chamber and interfaced to a computer. Various sample configurations have been utilized and were described in detail elsewhere.[9]

b. Infrared Spectroscopy. Fourier transform infrared (FTIR) spectroscopy was performed simultaneously with dielectric measurements using a setup described elsewhere.[10]

Results and Discussion

Near-Infrared and Mid-Infrared Fourier Transform Spectroscopy. We begin our discussion by presenting the results of near-infrared (NIR) and mid-infrared (MIR) spectroscopy obtained in situ during isothermal cure. Vibrational spectra provide information on the chemical and physical phenomena that accompany network formation by identifying the type and concentration of different chemical groups at various stages of cure, the interactions between them, and the reaction kinetics. First, we collected NIR data on our remote optical fiber assembly[12] and examined the reaction mechanism. Progressive changes in the spectra were systematic and conducive to a precise quantitative analysis. Trends displayed by the major peaks of relevance in epoxy/amine reactions were evident; a decrease in epoxy absorption (4,530 and 6080 cm^{-1}), a decrease in primary amine (4950 cm^{-1}) and primary and secondary amine (6500 cm^{-1}) absorptions, and an increase in hydroxyl absorption (around 7000 cm^{-1}). A comprehensive account of the origin, location, and shifts of all NIR peaks during epoxy/amine reactions is given elsewhere.[13]

Spectral data were used to determine the reaction kinetics at different temperatures, according to the methodology documented in the literature.[12,14] Extent of reaction, calculated from NIR data on the basis of the area under the epoxy peak at 4530 cm^{-1}, is shown as a function of reaction time with temperature as a parameter in Figure 2. This information was used later to obtain networks of the desired degree of cure. Further information about the molecular aspects of DGCDC−PACM cure was obtained from MIR measurements. We focused our attention on three types of specific interactions that directly affect the network dynamics during epoxy/amine cure: (1) dipole−dipole interactions which form between polar groups immediately after the ingredients (epoxy and amine) are mixed and which persist up to about 10% conversion; (2) interactions due to the hydrogen-bonded complexes

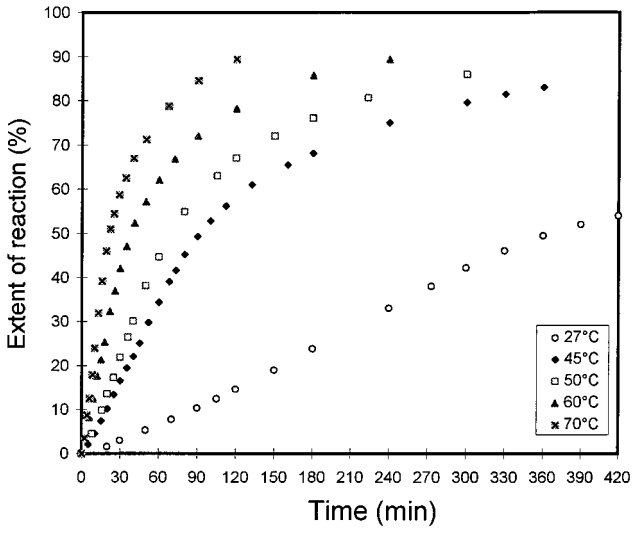

Figure 2. Extent of reaction as a function of reaction time with temperature as a parameter.

that form as the network grows and approaches the gel point;[10,14−16] (3) interactions that involve the carbonyl group and hence are characteristic of DGCDC−PACM formulations only. Our spectroscopic results did not reveal differences between DGEBA−MDA and DGCDC−PACM formulations in regards to either the reaction mechanism or the first two types of specific interactions, namely, dipole−dipole interactions and hydrogen-bonded complexes. Dipole−dipole interactions in the as-mixed nonreacted formulation impose conformational restrictions to the mobility of polar (dielectrically active) species and affect dynamics but are gradually relaxed during early cure. The presence of these interactions in nonreacted epoxy/amine formulations is manifested in the MIR and NIR spectra by an unusual *increase* in the intensity of amine absorption peaks during the first 10% conversion. This finding was common to all non-polymer-forming and polymer-forming epoxy/amine mixtures, including DGCDC−PACM formulation. Above 10% conversion, however, this trend is reversed and we observe a *decrease* in the amine absorption intensity, which mimics that of the epoxy group. The underlying mechanism of this phenomenon has been described elsewhere.[17] Another type of interaction has been observed in the vicinity of the gel point, which occurs at about 58% conversion in all bifunctional-epoxy/tetrafuctional-amine systems.[18] The appearance of these interactions is caused by the interplay of physical and chemical changes that set in as the network approaches the gel point. The physical change in the network is manifested as a decrease in the distance (densification) between polar groups in the reactive mixture, whereas the chemical change, which is a consequence of the ongoing chemical reactions, creates the right balance of reactants and products that ultimately leads to the formation of specific hydrogen-bonded complexes. The emergence of these complexes is contingent upon reaching a critical combined concentration of epoxy, amine, and hydroxyl groups; the nature of these complexes in the DGEBA-type epoxies has been discussed in more detail elsewhere[10,14,15] but has not been investigated in DGCDC-type epoxies prior to this study. We begin by examining the change in the epoxy absorption at 906 cm^{-1} during DGCDC−PACM cure, shown in Figure 3A,B. The numbers adjacent to each curve denote percent conversion. Below the gel point,

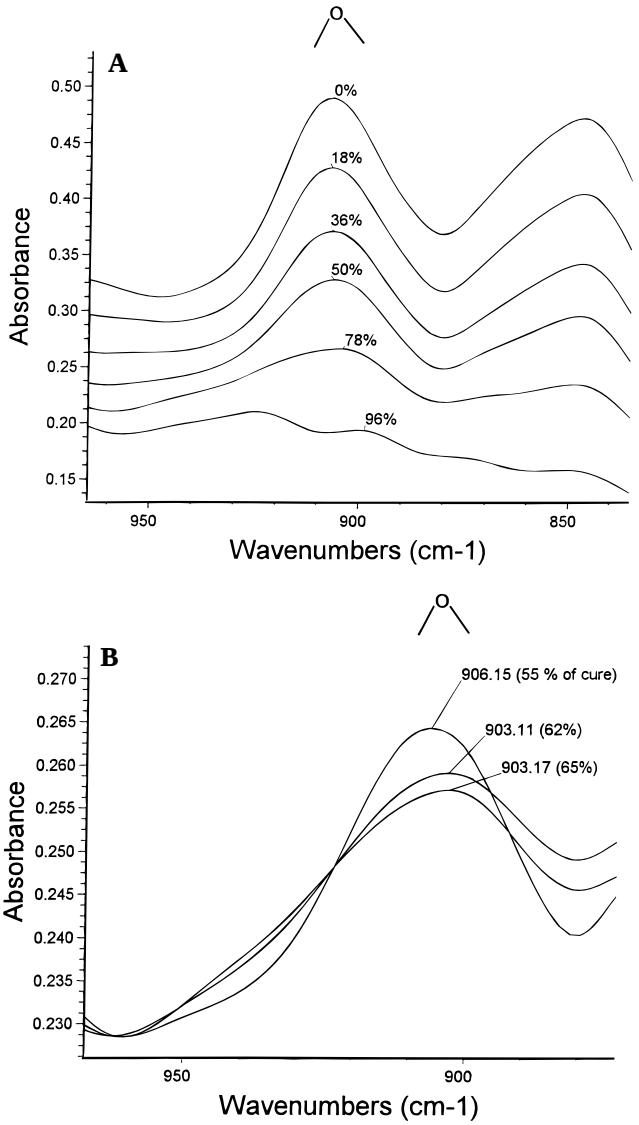

Figure 3. Changes in the epoxy absorption at 906 cm^{-1} during DGCDC−PACM cure: (A) percent conversion as a parameter; (B) peak maximum and percent conversion in parentheses.

the intensity of the epoxy peak decreases but the frequency at maximum stays unchanged. Figure 3B highlights the spectral region of the epoxy peak near the gel point. The formation of hydrogen-bonded complexes affects these spectra as follows: (1) the epoxy peak (initially located at 906 cm^{-1}) shifts to lower wavenumbers; (2) a new peak emerges at 925 cm^{-1}, as indicated by arrows in Figure 3A,B. In our earlier study of non-polymer-forming and polymer-forming epoxy/amine systems,[13−15] including DGEBA−MDA formulation, we have also identified a new peak, associated with hydrogen-bonded complexes, which emerges and increases in intensity during cure. However, the frequency at maximum for that peak overlapped considerably with that of the original epoxy peak, which is located in this formulation at 915 cm^{-1}, making it difficult to resolve the new peak quantitatively. Failure to recognize the emergence of this peak has led to erroneous estimates of the concentration of epoxy groups in the later stages of cure and has rendered unreliable a number of reports in the literature based on MIR measurements of epoxy cure kinetics *above* the gel point. An important finding here is that the difference in the molecular architecture of DGEBA and DGCDC epoxies

Chart 1. Proposed Intramolecular Hydrogen-Bonded Complex, Which Forms between Carbonyl and Hydroxyl Groups during DGCDC−PACM Network Formation

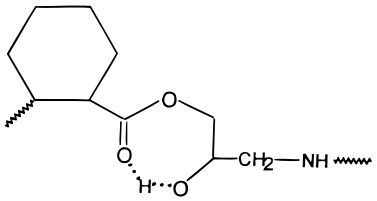

enables one to monitor the growth of a new peak at 925 cm^{-1} in the latter system. This amounts to an advantage in that we can now (1) deconvolute these two peaks and utilize the peak at 906 cm^{-1} to calculate the DGCDC−PACM reaction kinetics beyond the gel point as well and (2) detect the onset of formation of hydrogen-bonded complexes. The significance of the finding is that it amounts to a spectroscopic signature of gelation.

Hydrogen bonding that co-involves carbonyl groups is an important feature of DGCDC−PACM formulations, and we focus on the carbonyl group next. Changes in the carbonyl absorption at 1735 cm^{-1} during cure are monitored, and two characteristic trends are readily observed. First, we detect a gradual broadening of the lower frequency (lower wavenumber) side of the peak, indicating an increasing participation of carbonyl groups in hydrogen-bonding interactions. Interestingly, however, the total area under the peak stays unchanged, possibly as a consequence of the continuous interchange between the non-hydrogen-bonded and hydrogen-bonded carbonyl groups. The second characteristic trend is a pronounced shift of the peak maximum to lower frequency, which is first detected in the vicinity of the gel point. We interpret this as the evidence that carbonyl groups take an active part in these newly formed hydrogen-bonded complexes.

On the basis of the spectroscopic evidence, we believe that the intramolecular hydrogen-bonded complex given in Chart 1 forms between carbonyl and hydroxyl group during DGCDC−PACM cure. Stable 7-, 8-, and even 10-membered hydrogen-bonded complexes are known to exist (refs 19−21 and references therein). For example, the monoanion of maleic acid forms a stable 7-membered intramolecular hydrogen-bonded complex,[19] while ortho-substituted phenols have been shown to form 10-membered rings.[20] Among polymers, tetranuclear novolaks were reported to form stable 8-membered intramolecular hydrogen-bonded rings.[21] An important property of the proposed 7-membered conformation in DGCDC−PACM networks is the enhanced dipole moment of the carbonyl unit, resulting from the interactions between the carbonyl oxygen and the hydroxyl hydrogen. Moreover, each hydroxyl hydrogen in the complex is strongly polarized and acts as a free positive charge that can move between the two oxygen atoms. When this active proton moves, the electron density shifts in the opposite direction, increasing the net positive charge. A hypothesis that this would have an effect on dipole dynamics in DGCDC−PACM systems during cure was investigated by DRS, and these results are described next.

Dielectric Relaxation Spectroscopy. In this section we present the results of dielectric measurements on DGCDC−PACM formulation at various stages of network formation. The measurements were performed in the frequency and temperature domain. Dielectric data in the frequency domain were collected by performing (a) continuous frequency sweeps during an isothermal reaction and (b) frequency sweeps on partially cured samples under conditions where no chemical reactions take place. The analysis of network dynamics was conducted by investigating the location, intensity, frequency dependence, and temperature dependence of the most probable relaxation time, τ, and the breath and shape of the relaxation spectrum. We shall first present and discuss the results obtained *during* network formation (cure) and then the results obtained on *partially cured* networks. Finally, we shall describe an attempt to correlate molecular dynamics and chemical kinetics during the network formation.

DRS during Network Formation. Our initial effort was aimed at understanding how the progress of chemical reactions affects the dynamics of two major relaxation processes in the frequency domain, namely, α and β, whose salient features are recapped below. α relaxation is the major dielectric relaxation in materials with permanent dipoles, and its origin lies in segmental motions, while β relaxation is associated with localized motions. It is important to point out that (1) α and β relaxations have different length scales but are interrelated since usually the same dipoles contribute to both processes and (2) α and β relaxations merge at high temperature (and high frequency) to give rise to an $\alpha\beta$ process. The pioneering work in describing the total time domain relaxation function for the $\alpha\beta$ process in terms of the contributions from the normalized relaxation functions for α and β processes was done by Williams.[22] Subsequent studies of the coalescence/splitting and the physical origin of the $\alpha\beta$ process have been reported (e.g., refs 23−26), but none examined the system whose structure changes as a result of chemical reactions until a recent work by Casalini et al.[27] An excellent study of the temperature dependence of α and β processes in an epoxy prepolymer was also reported by Casalini et al.[28]

Our previous work on epoxy/amine formulations has established that α relaxation is caused by the segmental motions of terminal epoxy groups on glycidyl moieties, while β relaxation arises from the localized motions within the epoxy ring. Of interest here was to establish how α and β relaxations vary during network formation. In Figure 4 we plot dielectric loss in the frequency domain at various stages of cure at 60 °C. In the as-mixed (0% conversion) formulation at that temperature, the α and β processes merge and we observe a single $\alpha\beta$ relaxation with a maximum at 2 GHz. With the advancement of reactions (see Figure 4), α and β relaxations begin to separate out: α relaxation shifts gradually to a lower frequency as a consequence of the increase in the glass transition of the growing network, while β relaxation, because of its localized origin, is little affected by the network growth and the location of this peak remains practically unchanged. Solid lines in Figure 4 represent fits to the Havriliak−Negamy (H−N) equation,[29] with a conductivity term included to describe the low-frequency end of dielectric loss. No further attempts were made to relate the adjustable H−N parameters to the characteristics of growing networks.

Figure 5 shows the real part of complex permittivity (which is referred to as the "dielectric constant" throughout the text) in the frequency domain with conversion (reaction time) as a parameter during DGCDC−PACM

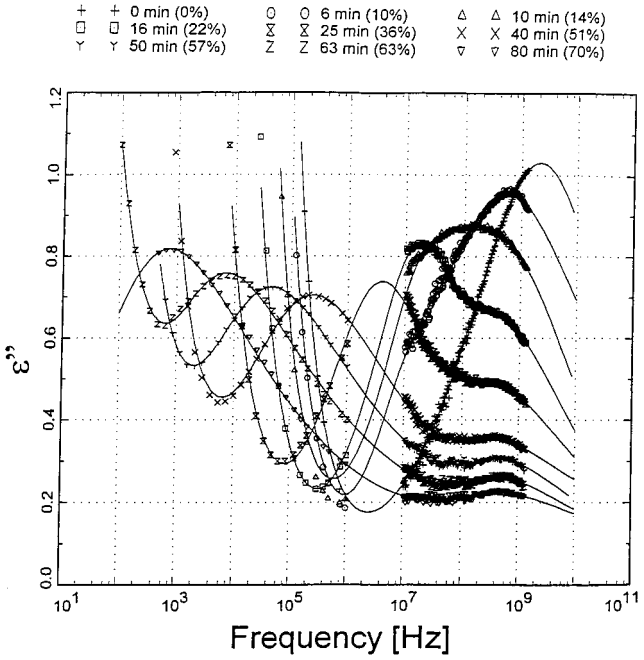

Figure 4. Dielectric loss in the frequency domain with reaction time (percent conversion) as a parameter during DGCDC−PACM cure at 60 °C.

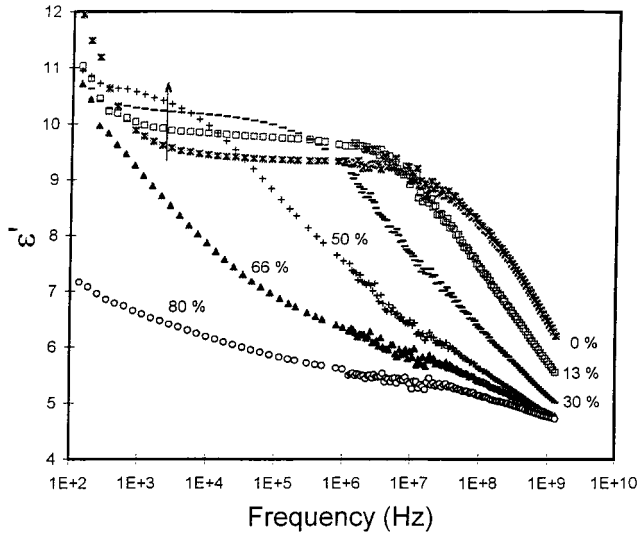

Figure 5. Dielectric constant in the frequency domain with percent conversion as a parameter during DGCDC−PACM cure at 50 °C.

cure at 50 °C. Extent of reaction was determined by remote fiber-optic NIR measurements, and these results were already displayed in Figure 2. An interesting result is the observed *increase* (indicated by an arrow at about 2 kHz in Figure 5) in the relaxed (limiting low-frequency) dielectric constant during reaction. Since the unrelaxed (limiting high-frequency) dielectric constant stays practically unchanged during cure, this implies that the dielectric dispersion increases as well. An important point is that the observed change is a characteristic of the reactive mixture and not of either component alone. This is witnessed by the fact that the dielectric constant of DGCDC or PACM does not change with time, while that of the reactive formulation increases steadily during cure up to vitrification. We note that the same trend in the dielectric constant was observed in a mixture of DGCDC and a different

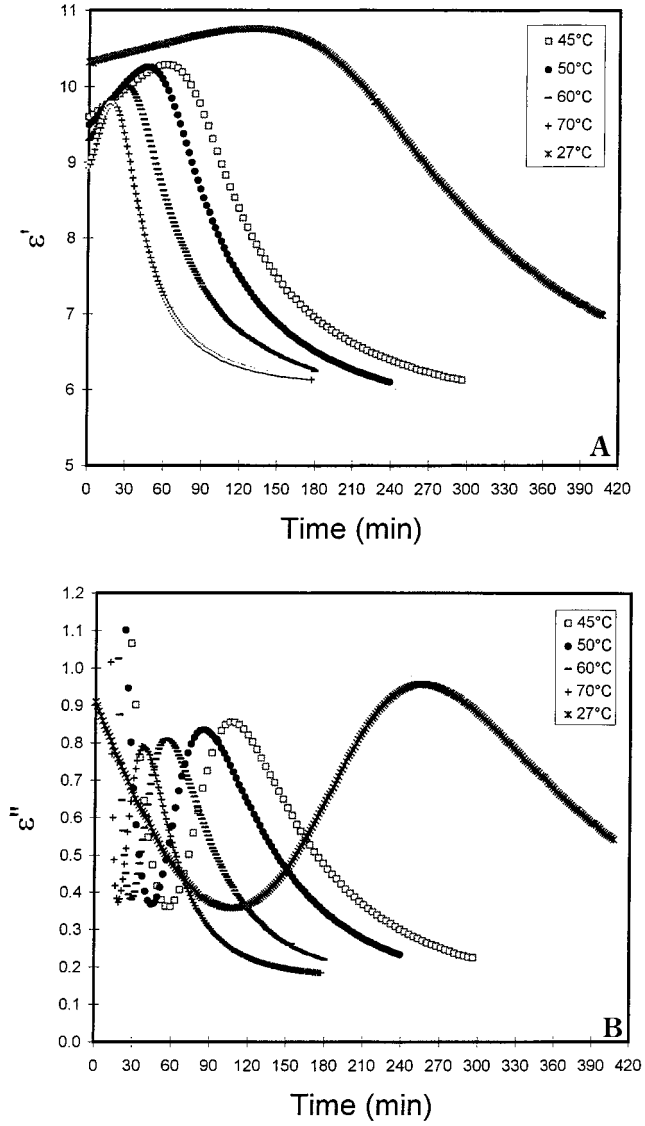

Figure 6. (A) Dielectric constant as a function of reaction time at 25 kHz with temperature as a parameter. (B) Dielectric loss as a function of reaction time at 25 kHz with temperature as a parameter.

hardener (MDA), providing additional evidence that the molecular architecture of the epoxy prepolymer itself is responsible for this phenomenon. We therefore conclude that this behavior is unique to DGCDC prepolymer and in contrast with various other epoxy/amine formulations,[30−33] where a *decrease* in the limiting low-frequency dielectric constant is observed and often used to correlate the dielectric response with the concentration of epoxy groups and the kinetics of cure.

This unexpected initial increase in the dielectric constant and dielectric dispersion during cure is seen even more clear in the plots at single frequency (25 kHz) and various temperatures, shown in Figure 6A, where we observe that (1) a steady increase in the dielectric constant accompanies cure at every temperature from the onset of reaction to vitrification and (2) the rate of change of the dielectric constant with reaction time (i.e., the slope) increases with increasing temperature. Changes in dielectric loss for the same reaction conditions are included for completeness in Figure 6B. As shown earlier (Figure 2), extent of reaction also increases with time during DGCDC−PACM cure up to

approximately 50% conversion, suggesting the possibility that the kinetic information obtained from DRS and NIR measurements could be related. Such an attempt was made as a part of a broader study of the relationship between molecular dynamics and chemical kinetics and is described later in the text.

An interesting question is whether the dielectric constant of the DGCDC−PACM formulation is the *only* physical property of this system that changes during cure in a manner so different from the various DGEBA-type formulations. This question was addressed by comparing the change in ionic conductivity up to the gel point during DGCDC−PACM and DGEBA−MDA cure. Although the extrinsic ionic conductivity does not contribute to the dielectric constant (it contributes to loss only), the intrinsic contributions to the overall conductivity were shown to have a strong effect in some epoxy/amine formulations.[34] Using the methodology documented in the literature,[35,36] ionic conductivity was calculated and found to decrease steadily in the course of network formation, just like in the DGEBA−MDA formulation.[37]

What then causes the observed increase in the dielectric constant during DGCDC−PACM cure? We believe that an explanation should be sought in terms of the total dipole moment of the reactive mixture. Let us begin by reiterating that the segmental motions of glycidyl units with terminal epoxy groups are predominately responsible for the α process and as such provide a major contribution to the dielectric constant. In that case, one would intuitively expect the limiting low-frequency dielectric constant to decrease during cure because it is dominated by the contributions from the mean-square dipole moment of glycidyl units, which, in turn, are consumed by chemical reactions in the course of network formation. While this is true for DGEBA-type epoxies, in DGCDC-type epoxies we see the opposite trend, caused by the contribution of carbonyl groups to the overall dipole moment in the form of carbonyl−hydroxyl intramolecular hydrogen-bonded complexes, depicted in Chart 1, which form continuously during reaction. The ensuing 7-membered ring is an energetically favorable conformation which increases the asymmetry of charge distribution and hence the dipole moment of a carbonyl group. This provides an additional contribution to the average mean-square dipole moment which outweighs the opposite effect caused by the consumption of epoxy groups, resulting in an increase in the limiting low-frequency permittivity during cure. The change in the mean-square dipole moment during cure is important though not easily obtainable. In an earlier study of a model epoxy/amine (two-step condensation) system,[9] we found that the dielectric constant drops from about 10 to 3 (relaxation strength, $\Delta\epsilon' = 7$) as the unreacted mixture undergoes α relaxation. In the same system upon the completion of reaction we find $\Delta\epsilon' = 1$. Assuming direct proportionality between the dielectric constant and the mean-square dipole moment, one could conclude that the conversion of initial reactants into products is accompanied by a 7-fold decrease in the average mean-square dipole moment. In the multifunctional epoxy/amine formulations, however, such an analysis is more complex. In the DGCDC−PACM formulation we observe initially ("as-mixed", 0% conversion) a decrease in ϵ' from about 9.5 to 4.5; hence, $\Delta\epsilon' = 5$. The relaxation strength increases during reaction ($\Delta\epsilon' = 5.5$ at 13%; 5.8 at 30%; 6.3 at 50%) but the α process shifts to lower frequencies with further cure, making the determination of $\Delta\epsilon'$ difficult. There is an additional mechanism that could possibly affect the overall dipole moment. It was also shown earlier[9,10] that the contribution of hydroxyl and secondary amine dipoles to the α process in the DGEBA−MDA formulation was small, in part because of the opposite direction of these two dipole moments that act to cancel each other. In the DGCDC−PACM formulation, however, this assumption does not hold anymore because the direction of the hydroxyl dipole moment has been altered because of the intramolecular association with the carbonyl group.

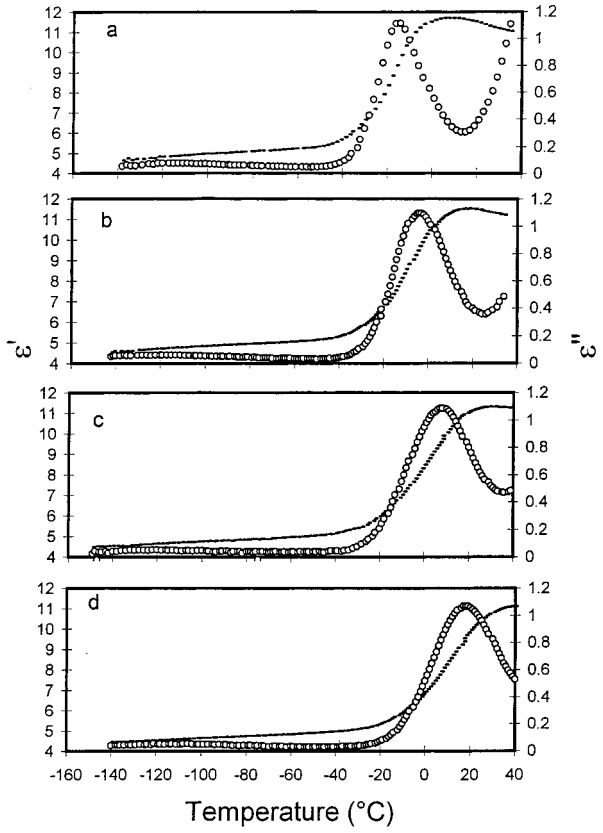

Figure 7. Dielectric constant and loss as a function of temperature for networks partially cured to (a) 0, (b) 10, (c) 20, and (d) 30% conversion.

DRS of Partially Cured Networks. The following procedure was used to investigate the reorientational dynamics of partially cured networks. Samples were cured isothermally to a desired conversion (monitored by NIR), quenched below the glass transition temperature to arrest the reactions, and then tested under the conditions where no further cure took place. The dynamics of partially cured networks were investigated by analyzing the most probable relaxation time and the relaxation spectrum of the α process. Although this type of analysis was feasible only up to 30% conversion, interesting results were obtained. Samples cured to higher conversion could not be examined because the cure would resume quickly above the glass transition temperature of the partially cured network. In Figure 7a−d we plot the dielectric constant and loss as a function of temperature for networks partially cured to (a) 0%, (b) 10%, (c) 20%, and (d) 30% conversion. Several characteristic features are readily observed: (1) a systematic shift of the α relaxation peak to higher temperature, as a result of the decreased molecular

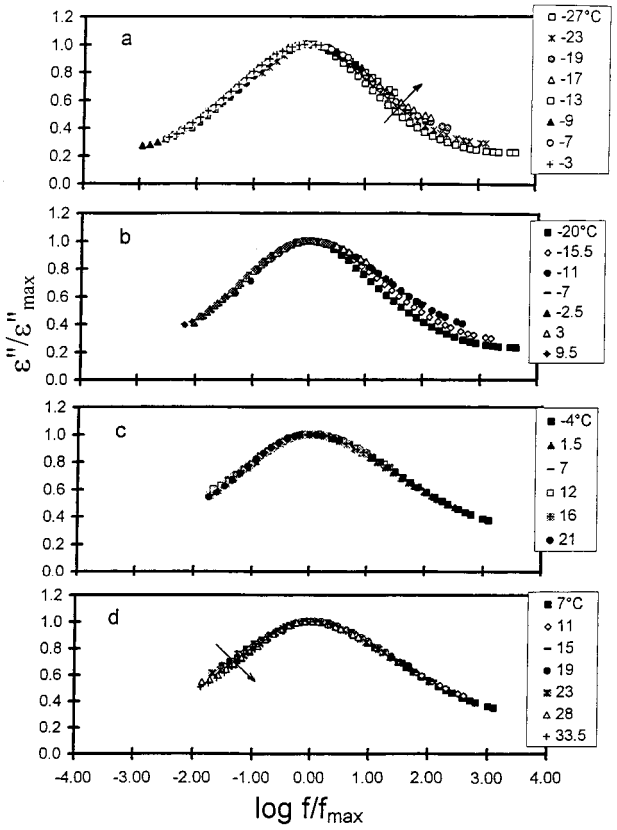

Figure 8. Normalized dielectric loss as a function of normalized frequency for networks at (a) 0, (b) 10, (c) 20, and (d) 30% conversion.

mobility (higher T_g), (2) a broadening of the dielectric loss peak, and (3) a very small change in the intensity of the dielectric dispersion with cure.

We next analyzed the α process in the frequency domain by conducting frequency sweeps of partially cured networks at various temperatures. In Figure 8a−d we show normalized dielectric loss as a function of normalized frequency for networks at 0%, 10%, 20%, and 30% conversion. The nonreacted sample (Figure 8A) shows a thermodielectrically simple behavior on the lower frequency side and a systematic broadening with increasing temperature on the higher frequency side of the normalized relaxation peak. At 10% conversion (Figure 8b) we again observe a thermodielectrically simple response for the long relaxation time processes. On the shorter time scale, however, a thermodielectrically complex response is observed only for the two lowest temperatures. A 20% cured sample (Figure 8c) showed thermodielectrically simple behavior on both sides of the spectrum. Surprisingly, a network at 30% conversion (Figure 8d) displayed a complex response only at the lower frequency side. The direction of these changes with increasing temperature in the networks at 0 and 30% is shown by arrows in parts a and d of Figure 8, respectively. It is difficult to rationalize these findings; if we assume that the thermodielectric complexity is a consequence of the presence of another relaxation, our data would suggest that the α process is affected by another process which traverses the spectrum from high to low frequency in these early stages of cure. Moreover, this other process is shifting to higher frequency with increasing temperature (see arrows in Figure 8a,b), suggesting a process with higher apparent activation energy. At present we are not sure what the underlying molecular nature of these phenomena is and are continuing to look into it.

Finally, plots of most probable relaxation time versus reciprocal temperature were constructed (not shown here) and used to calculate the apparent activation energy of the α process in the frequency range from 100 Hz to 1 MHz for networks at various stages of cure. The trends observed in the DGCDC−PACM formulation parallel those seen in other multifunctional epoxy networks.[10] The nonreacted (0%) sample showed a characteristic non-Arrhenius form which was attributed to the specific dipole−dipole interactions that form immediately upon mixing. Around 10% conversion these interactions are weakened and an Arrhenius response is observed. At higher conversion we detect a small but measurable increase in the apparent activation energy for the DGCDC−PACM network: 38.0 kcal/mol (at 10% conversion), 38.8 kcal/mol (20%), and 40.0 kcal/mol (30%). This finding is also in agreement with the results for several DGEBA-type epoxy/amine formulations.[10]

Correlations of Molecular Dynamics and Chemical Kinetics during Network Formation. As previously stated, fundamental studies aimed at correlating dipole dynamics with the kinetics of network formation are scarce. In our opinion, the most comprehensive effort reported thus far is due to Fournier et al.,[7] who utilized DRS and DSC to study the change in molecular dynamics during bulk polymerization of a DGEBA−PACM formulation. Our goal here was to build upon the methodology proposed by these authors and develop quantitative correlations between a processing parameter (the degree of cure, α) and a characteristic structural parameter (the most probable relaxation time, τ) during DGCDC−PACM cure. In the course of this analysis, however, we have introduced several novel steps that led to an improved methodology. First, we measured the advancement of cure in real time by *simultaneous* remote fiber-optic NIR and DRS, which eschews the use of off-line methods. Second, we employed an autocatalytic kinetic equation that had been successfully used in a series of studies of epoxy/amine kinetics by our group.[43,44] Third, we utilized a wider range of frequency (up to 12 decades in some instances) than those in any previously reported study of this kind. Fourth, we tested an epoxy/amine formulation which showed, as described earlier, an unusual increase in the limiting low-frequency relaxed permittivity during cure. Changes in molecular dynamics and chemical kinetics were analyzed according to the methodology whose salient features are recapped below.

The frequency of maximum loss, f_{max}, is related to the most probable relaxation time, τ, by

$$f_{max} = 1/(2\pi\tau) \quad (1)$$

An increase in the molecular weight and the cross-link density during network formation is accompanied by a concomitant decrease in the molecular mobility and an increase in the average relaxation time. An exponential dependence of the most probable relaxation time on reaction time, although phenomenological, affords a good description of the process, and hence we write

$$\tau = \tau_0 \exp(kt_{max}) \quad (2)$$

or

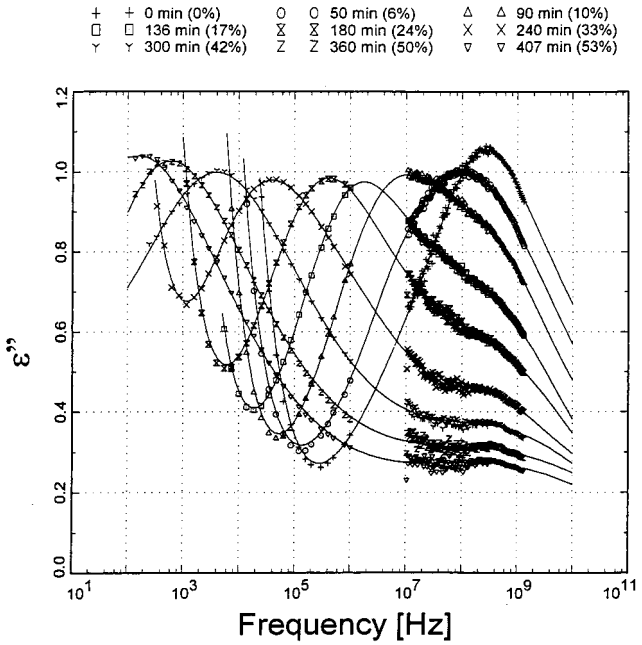

Figure 9. Dielectric loss in the frequency domain with reaction time (percent conversion) as a parameter during DGCDC−PACM cure at 28 °C.

$$f_{max} = f_{max}(0)\exp(-kt_{max}) \tag{3}$$

where the time of maximum dielectric loss, t_{max}, is chosen to define an operational reaction time with respect to the measuring frequency, $f_{max}(0)$ is the frequency of the maximum loss for the uncured material, and k is a constant for a given reaction temperature. The next step is to introduce kinetic information into eq 3. First we write the rate of polymerization, $d\alpha/dt$, in the following general form:

$$\frac{d\alpha}{dt} = kf'(\alpha)f''(\alpha) \tag{4}$$

where $f'(\alpha)$ defines the kinetic expression and $f''(\alpha)$ is the diffusion control factor. Equation 4 can be rewritten to yield the time $t(\alpha)$ needed to reach a given extent of reaction:

$$t(\alpha) = \int_0^\alpha \frac{d\alpha}{f'(\alpha)f''(\alpha)} \tag{5}$$

When eqs 3 and 5 are combined, the frequency at maximum loss for a fixed reaction temperature can be expressed as a function of the degree of cure as follows:

$$\ln f_{max} = \ln f_{max}(0) - k\int_0^\alpha \frac{d\alpha}{f'(\alpha)f''(\alpha)} \tag{6}$$

Equation 6 relates molecular dynamics to chemical kinetics. In the conversion range where diffusion control is absent, the second term under the integral is equal to unity ($f''(\alpha) = 1$).

We begin our analysis by examining plots of dielectric loss in the frequency domain as a function of reaction time (conversion) at 27 and 60 °C, shown in Figures 9 and 4, respectively. Frequency sweeps were obtained over a range from 100 Hz to 1.3 GHz. A comparison of the loss intensity at 27 and 60 °C indicates that the strength of the α process decreases, while that of the β process increases with increasing temperature. Solid lines in Figures 4 and 9 are fits to the Havriliak−Negamy equation which describes α and β relaxations and the low-frequency conductivity. The frequency at maximum loss was obtained from each scan at the reaction time where the degree of cure is known from the simultaneous NIR measurement.

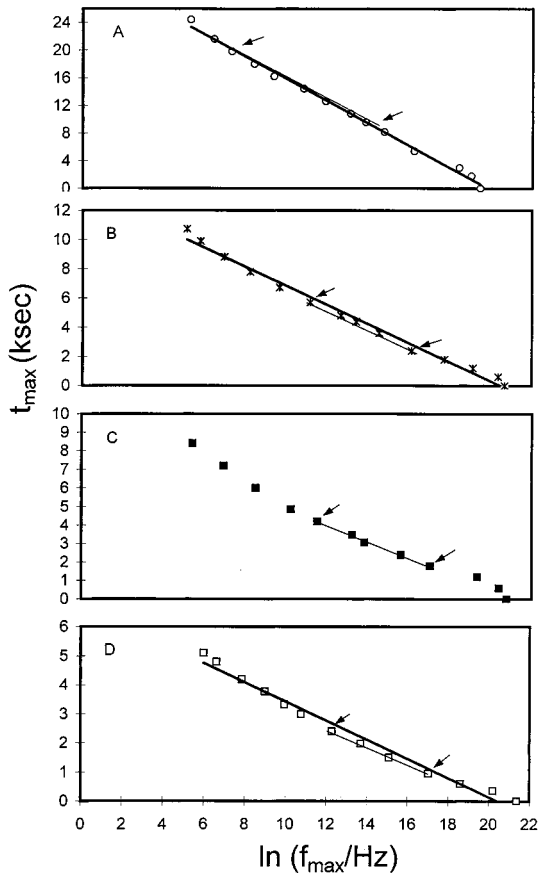

Figure 10. Time of maximum loss as a function of ln f_{max} for the following reaction temperatures: (A) 27, (B) 45, (C) 50, and (D) 60 °C. Arrows indicate the linear portion used in eq 2.

By rearranging eq 3 and expressing the time at maximum loss, t_{max}, as a function of ln f_{max}, we obtain

$$t_{max} = -\frac{1}{k}\ln f_{max} + \frac{1}{k}\ln f_{max}(0) \tag{7}$$

If this relationship is valid, then the plots of t_{max} as a function of ln f_{max} should yield a straight line. However, when one examines data over a wide range of frequency and temperature, it becomes immediately clear that eq 7 oversimplifies the situation and that the relationship between t_{max} and ln f_{max} is more complex. Figure 10A−D contain plots of the time of maximum loss as a function of ln f_{max} at the following temperatures: (A) 27; (B) 45; (C) 50; and (D) 60 °C. A linear relationship was found *in all runs between 20 and 50% conversion*, and that range is marked by arrows in Figure 10. Outside this common range, however, the curves exhibit different behavior. Interestingly, the shape of curves A−D over the entire conversion range is almost identical, suggesting similar dynamics in DGCDC−PACM networks cured at different temperatures. In principle, to utilize a relationship between t_{max} and ln f_{max} as the working hypothesis over the entire conversion range, one must formulate a chemophysical model based on a fundamental description of (1) the increase in the glass

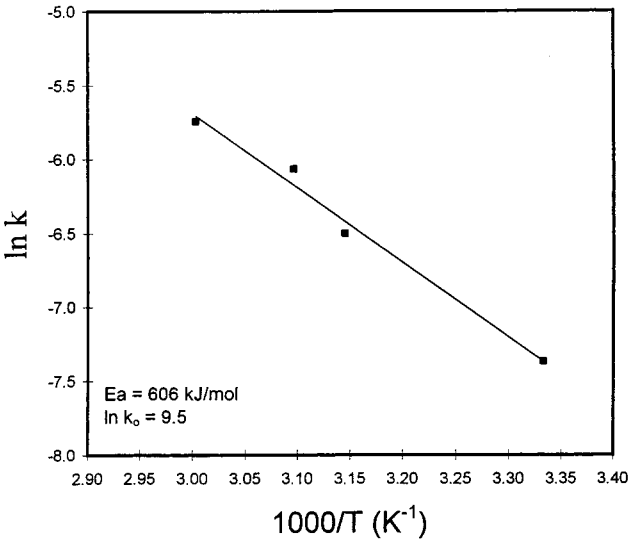

Figure 11. Arrhenius plot of the rate (time) constant as a function of reciprocal temperature.

Table 1. Kinetic Parameters of Equation 7

T (°C)	$f_{max}(0)$ (GHz)	$k \times 10^3$ (1/s)	T (°C)	$f_{max}(0)$ (GHz)	$k \times 10^3$ (1/s)
27	0.44	0.63	50	1.5	2.1
45	0.41	1.5	60	4.4	3.1

transition temperature during network formation, (2) the increase in the most probable relaxation time during network formation, (3) the nature and splitting of the $\alpha\beta$ process, and (4) a continuous change in the apparent activation energy (within the frequency interval where the Arrhenius form is observed) for the α process during cure. In the absence of such a model, we limit our discussion here to network dynamics in the conversion range corresponding to the linear portion of Figure 10A−D. From the slope and intercept we obtain k and the frequency of maximum loss for the uncured material, $f_{max}(0)$, for each temperature. Both k and $f_{max}(0)$ increase with increasing temperature. These data are summarized in Table 1 and will be used later in eq 6. A plot of k as a function of reciprocal temperature, shown in Figure 11, yields a straight line and can be described by

$$k = k_0 \exp\left(\frac{-E_a}{RT}\right) \tag{8}$$

where E_a is an apparent activation energy, R the gas constant, and k_0 the preexponential factor. The calculated values of $\ln(k_0) = 9.5$ and $E_a = 606$ kJ/mol are similar to those reported for DGEBA−PACM cure.[7]

The next step was to examine further the NIR kinetics for the DGCDC−PACM system (Figure 3), with the goal of (1) developing a kinetic expression that could describe cure in the chemically controlled regime and (2) identifying the stage where diffusion control takes over. This was accomplished utilizing a procedure described by Martin.[38] Figure 12 was obtained by shifting the conversion−time curves at various temperatures to superimpose with the curve at an arbitrary reference temperature, in this case 50 °C. The shift factor for this procedure was determined by a "univariable search", designed to minimize the difference between the actual cure time at 50 °C and the equivalent cure time at another reaction temperature. The term univariable implies that a single constant is sufficient to superpose data in the chemically controlled cure regime. Interestingly, using this methodology, we found no evidence of diffusion control up to 90% conversion, as shown in Figure 12. This is different from the trend observed in DGEBA-type epoxies, where diffusion control sets in soon after gelation.[38,39] An explanation could be offered, at least partly, in terms of the difference in the molecular architecture of the formulation components, e.g., cyclohexyl (DGCDC, PACM) versus benzene ring (DGEBA, MDA), etc. The cyclohexyl ring imparts additional flexibility to the networks and lowers its $T_{g\infty}$ (T_g at 100% conversion).

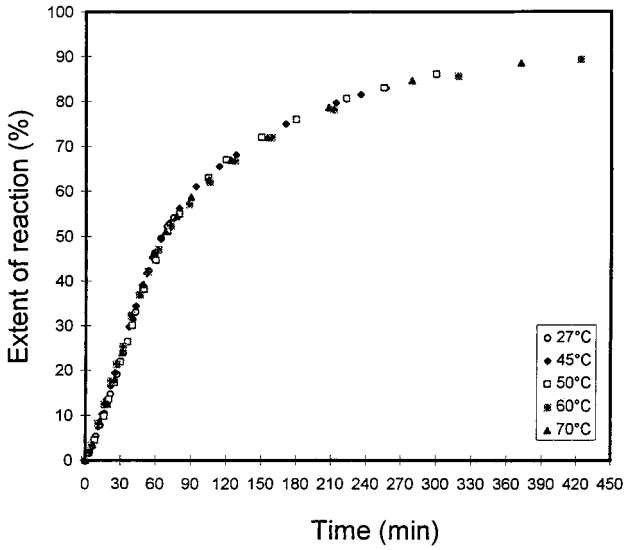

Figure 12. Extent of reaction as a function of equivalent cure time at 50 °C.

Table 2. Reaction Rate Constants of Equation 9

T (°C)	$k_1 \times 10^5$ (1/s)	$k_2 \times 10^4$ (1/s)	T (°C)	$k_1 \times 10^5$ (1/s)	$k_2 \times 10^4$ (1/s)
27	0.411	1.42	60	13.4	6.37
45	4.01	3.05	70	19.2	12.5
50	4.16	4.51			

Assuming that diffusion control does not affect kinetics at the conditions of Figure 12, we proceeded to seek a kinetic expression that could fit the experimental data. An early study by Horie et al.[40] led to the development of a mechanistic model for epoxy/amine kinetics. Horie's model was later modified by Kamal,[41] who proposed the following phenomenological kinetic expression:

$$\frac{d\alpha}{dt} = (k_1 + k_2\alpha^n)(1 - \alpha)^m \tag{9}$$

where α is the extent of reaction, k_1 and k_2 are reaction rate constants, and the sum $m + n$ is the overall reaction order. The autocatalytic nature of epoxy/amine kinetics is now well recognized, and eq 9 has been successfully employed in many studies of epoxy/amine kinetics:[42−45] Solid lines in Figure 13 were calculated using eq 9, and the best fits were obtained with the values of $n = 0.5$ and $m = 2$. Kinetic rate constants k_1 and k_2 are obtained as adjustable parameters, and their values are summarized in Table 2 for several reaction temperatures. Both rate constants were found to obey the Arrhenius law. Particularly good linear correlation was observed for k_2, whose apparent activation energy (612

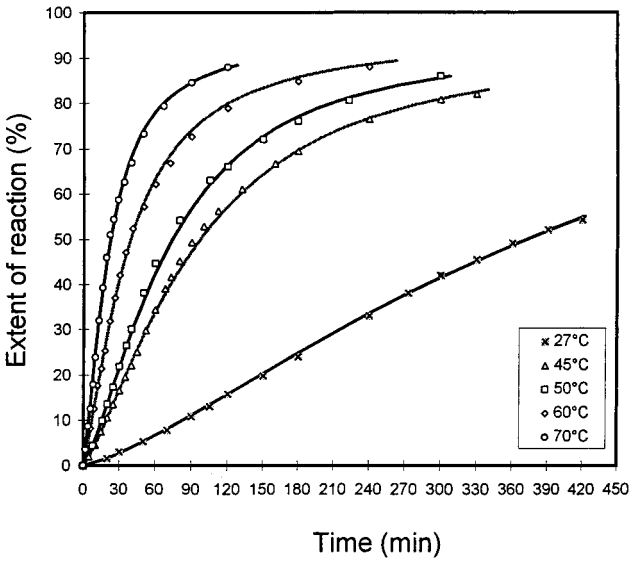

Figure 13. Extent of reaction as a function of reaction time with temperature as a parameter. Solid lines are fits to eq 10.

kJ/mol) was close to the value (606 kJ/mol) obtained from time constant k (eq 8) from DRS.

Next, we evaluate the integral in eq 6 by substituting $f'(\alpha)$ with eq 9 and setting $f''(\alpha) = 1$. Time at a given conversion was calculated from the following analytical expression:

$$t(\alpha) = \frac{1}{12}\left[\frac{1}{k_1} + \frac{1}{(k_1 + k_2\alpha^n)(1-\alpha)^m} + 4\left(\sum_{i=1}^{2}\frac{1}{\left(k_1 + k_2\left(\frac{1}{4}(2i-1)\alpha\right)^n\right)\left(1-\frac{1}{4}(2i-1)\alpha\right)^m}\right)\right] + \frac{1}{6}\left(\sum_{i=1}^{1}\frac{1}{\left(k_1 + k_2\left(\frac{1}{2}i\alpha\right)^n\right)\left(1-\frac{1}{2}i\alpha\right)^m}\right) \quad (10)$$

where $n = 0.5$ and $m = 2$. By substituting eq 10 into eq 6, we obtain a relationship that connects the frequency of maximum loss, f_{max} (or the most probable relaxation time, since $\tau = (2\pi f_{max}) - 1$), with extent of reaction, α. Plots of ln f_{max} versus α are shown in Figure 14 for several reaction temperatures. Solid lines are calculated values from eq 6. Although eq 7 satisfies only a limited experimental range, we observe good fits. The largest discrepancy is observed at the onset of reaction where the dielectric response is affected by the splitting of α and β processes.

An alternative route to relating the degree of cure with the frequency of maximum loss was also presented by Fournier et al.[7] They studied DGEBA−PACM cure and found that over a certain conversion range plots of ln f_{max} versus α were linear and could be approximated by the following equation:

$$f'_{max} = f'_{max}(0)\exp(-k_a\alpha) \quad (11)$$

where k_α is rate a constant and other symbols are as previously defined. A correlation between the frequency at maximum loss and cure kinetics, which includes the diffusion control term, was given as

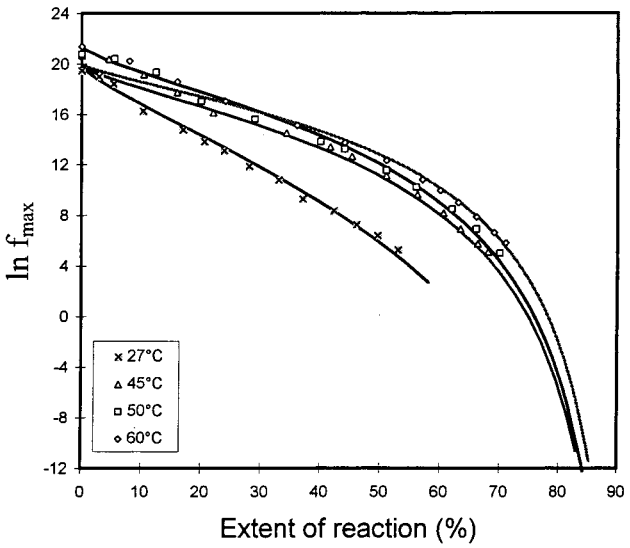

Figure 14. ln f_{max} as a function of extent of reaction with temperature as a parameter. Solid lines are calculated from eq 5.

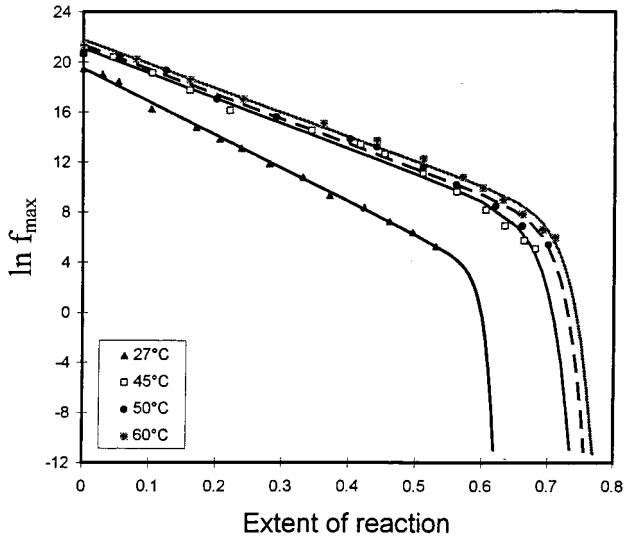

Figure 15. ln f_{max} as a function of extent of reaction with temperature as a parameter. Solid lines are fits to eq 13.

Table 3. Kinetic Parameters of Equation 12

T (°C)	$a(T)$	$c(T)$	b	k_α	$f'_{max}(0)$ (GHz)	α_f
27	104	−1965	0.0144	0.258	0.21	0.70
45	116	−2341	0.0296	0.174	0.69	0.90
50	115	−2356	0.0275	0.173	0.89	0.91
60	112	−2358	0.0289	0.174	1.7	0.93

$$\ln f'_{max} = a(T)\,[\ln f'_{max}(0) - k_\alpha\alpha]x\left[\frac{2}{1+\exp\left(\frac{\alpha-\alpha_f}{b}\right)} - 1\right] + c(T) \quad (12)$$

where α_f is the final degree of cure obtainable at a given temperature and b, $a(T)$, and $c(T)$ are adjustable parameters that depend on temperature. Equation 12 was then used to construct a series of plots of log f_{max} against extent of reaction. We repeated the same procedure for the DGCDC−PACM system. Fits of data to eq 12 are shown in Figure 15, and the corresponding kinetic parameters are summarized in Table 3. We find that

this expression does not provide a good description of the later stages of DGCDC−PACM cure because the bracketed term in eq 12, which accounts for diffusion control, consistently underestimates the final conversion at vitrification as determined from NIR data.

Conclusions

We have investigated the effect of insertion of a carbonyl group between the ether oxygen and the cyclohexyl ring of an epoxy prepolymer on the reorientational dynamics of epoxy/amine networks during cure.

Hydrogen-bonding interactions were shown to form during cure. A particularly pronounced change in the epoxy and carbonyl IR absorption peaks in the vicinity of the gel point provides a spectroscopic signature of gelation. It was proposed that a 7-membered intramolecular hydrogen-bonded complex that co-involves carbonyl and hydroxyl groups forms during cure.

Dynamics of the initial liquid DGCDC−PACM mixture are characterized by an $\alpha\beta$ process whose most probable relaxation time is on the order of picoseconds. In the course of network formation, however, α and β processes begin to separate out; α relaxation shifts gradually to a lower frequency as a result of the increase in the network glass transition, while the location of β relaxation remains largely unaffected by cure. An intriguing increase in the relaxed (limiting low-frequency) dielectric constant was observed during cure. A similar trend was absent in other multifunctional epoxy/amine formulations, indicating that the reason for this unusual behavior can be traced to the presence of carbonyl groups and their interactions in the network.

Frequency sweeps of partially cured networks at various stages of cross-linking below the gel point were used to construct plots of normalized dielectric loss against normalized frequency. The observed thermodielectric complexity followed a unique trend as a function of the degree of cure but was difficult to rationalize.

Finally, a correlation was worked out between molecular dynamics and cure kinetics during DGCDC−PACM cure. Modifications introduced to the framework proposed by Fournier et al.[7] led to an improved methodology. Good correlation was observed in the conversion range between 20 and 50%, despite the lack of a fundamental chemophysical model for network formation.

Acknowledgment. This material is based on work supported by the National Science Foundation under Grant No. DMR 9710480.

References and Notes

(1) Extensive accounts of relaxation in glass-forming liquids and amorphous polymers can be found in three special volumes of *J. Non-Cryst. Solids* (**1988**; 255−257; **1998**; 172−174; **1991**; 131−133) and in a special issue of *J. Res. Natl. Inst. Sci. Technol*. 102 (**1997**, *102*).
(2) Kranbuehl, D. E.; Delos, S. E.; Jue, P. K. *Polymer* **1986**, *27*, 11.
(3) Lane, J. W.; Seferis, J. C. *J. Appl. Polym. Sci.* **1986**, *31*, 1155.
(4) Senturia, S. D.; Sheppard, N. F. *Adv. Polym. Sci.* **1986**, *80*, 1.
(5) Mangion, M. B. M.; Johari, G. P. *J. Polym. Sci., Part B: Polym. Phys. Ed*. **1991**, *29*, 1127.
(6) Marugan, M. M.; Shinton, S.; Williams, G. *J. Mater. Chem*. **1996**, *6*, 667.
(7) Fournier, J.; Williams, G.; Duch, C.; Aldridge, G. A. *Macromolecules* **1996**, *29*, 7097.
(8) Williams, G. In *Dielectric Spectroscopy of Polymeric Materials;* Runt, J. P., Fitzgerald, J. J., Eds.; American Chemical Society: Washington, DC, 1997; Chapter 1, pp 3−65.
(9) Fitz, B.; Andjelic, S.; Mijovic, J. *Macromolecules* **1997**, *30*, 5227.
(10) Andjelic, S.; Fitz, B.; Mijovic, J. *Macromolecules* **1997**, *30*, 5239.
(11) Riande, E.; Saiz, E. *Dipole Moment and Birefringence of Polymers*; Prentice-Hall: Englewood Cliffs, NJ, 1992.
(12) Mijovic, J.; Andjelic, S. *Polymer* **1995**, *36*, 3783.
(13) Mijovic, J.; Andjelic, S. *Macromolecules* **1995**, *28*, 2789.
(14) Mijovic, J.; Andjelic, S. *Polymer* **1996**, *37*, 1295.
(15) Mijovic, J.; Andjelic, S.; Kenny, J. M. *Polym. Adv. Technol*. **1996**, *7*, 1.
(16) Mijovic, J.; Fishbain, A.; Wijaya, J. *Macromolecules* **1992**, *25*, 979.
(17) Andjelic, S.; Mijovic, J. *Macromolecules* **1998**, *31*, 2872.
(18) Flory, P. J. *Principles of Polymer Chemistry*; Cornell University Press: Ithaca, NY, 1953.
(19) Vinogradov, S. N.; Linnell, R. H. *Hydrogen Bonding*; Litton Educational Publishing: New York, 1971.
(20) Brzezinski, B.; Radziejewski, P.; Olejnik, J.; Zundel, G. *J. Phys. Chem*. **1993**, *97*, 6590.
(21) Scheiner, S. *Hydrogen Bonding*; Oxford Press: London, 1997.
(22) Williams, G. *Adv. Polym. Sci*. **1979**, *60*, 33.
(23) Donth, E. J. *Relaxation and Thermodynamics in Polymers: Glass Transition*; Akademie Verlag: Berlin, 1992.
(24) Garwe, F.; Schonhals, A.; Beiner, M.; Schröter, K.; Donth, E. *Macromolecules* **1996**, *29*, 247.
(25) Arbe, A.; Richter, D.; Colmenero, J.; Farago, B. *Phys. Rev. B* **1996**, *54*, 3853.
(26) Alvarez, F.; Hoffman, A.; Alegria, A.; Colmenero, J. *J. Chem. Phys.* **1996**, *105*, 432.
(27) Casalini, R.; Livi, A.; Rolla, P. A.; Levita, G.; Fioretto, D. *Phys. Rev. B* **1996**, *53*, 564.
(28) Casalini, R.; Fioretto, D.; Livi, A.; Lucchesi, M.; Rolla, P. A. *Phys. Rev. B* **1997**, *56*, 3016.
(29) Havrilliak, S.; Negami, S. *Polymer* **1967**, *8*, 161.
(30) Soualmia, A.; Huraux, C.; Despax, B. *Macromol. Chem*. **1982**, *183*, 1803.
(31) Sheppard, N. F.; Senturia, S. D. *Polym. Eng. Sci.* **1986**, *26*, 354.
(32) Parthun, M. G.; Johari, G. P. *J. Chem. Phys.* **1995**, *103*, 440.
(33) Levita, G.; Livi, A.; Rolla, P. A.; Culicchi, C. *J. Polym. Sci., Part B: Polym. Phys.* **1996**, *34*, 2731.
(34) Gallone, G.; Levita, G.; Mijovic, J.; Andjelic, S.; Rolla, P. A. *Polymer* **1998**, *39*, 2095.
(35) Mijovic, J.; Andjelic, S.; Yee, C. Y. W.; Bellucci F.; Nicolais, L. *Macromolecules* **1995**, *28*, 2797.
(36) Andjelic, S.; Mijovic, J.; Bellucci, F. *J. Polym. Sci., Part B: Polym. Phys.* **1998**, *36*, 641.
(37) Mijovic, J.; Bellucci, F.; Nicolais, L. *J. Electrochem. Soc*. **1995**, *142*, 1176.
(38) Deng, Y.; Martin, G. C. *Macromolecules* **1994**, *27*, 5147.
(39) Deng, Y.; Martin, G. C. *Macromolecules* **1994**, *27*, 5141.
(40) Horie, K.; Hiuro, H.; Sawada, M.; Mita, I.; Kambe, H. *J. Polym. Sci., Polym. Chem. Ed*. **1970**, *8*, 1357.
(41) Kamal, M. R. *Polym. Eng. Sci.* **1974**, *14*, 231.
(42) Rozenberg, B. A. *Adv. Polym. Sci*. **1986**, *75*, 113.
(43) Tanaka, Y.; Bauer, R. S. in *Epoxy Resin Chemistry and Technology*; May, C. A., Ed.; Marcel Dekker: New York, 1988.
(44) Mijovic, J.; Kim, J.; Slaby, J. *J. Appl. Polym. Sci.* **1984**, *29*, 1449.
(45) Moroni, A.; Mijovic, J.; Pearce, E. M.; Foun, C. C. *J. Appl. Polym. Sci.* **1986**, *32*, 3761.

MA980894W